STRAIN-MODULATED EPITAXY

FINAL PROGRESS REPORT

APRIL S. BROWN

September 8, 1999

U.S. ARMY RESEARCH OFFICE

CONTRACT NO: DAAH04-95-1-0367

GEORGIA INTSTITUTE OF TECHNOLOGY

APPROVED FOR PUBLIC RELEASE

DISTRIBUTION UNLIMITED

REPORT DOCUMENTATION PAGE

Form Approved
OMB NO. 0704-0188

1. AGENCY USE ONLY (Leave Blank)	2. REPORT DATE September 9, 1999	3. REPORT TYPE AND DATES COVERED Final Report

4. TITLE AND SUBTITLE
Strain-Modulated Epitaxy

5. FUNDING NUMBERS
DAAH04-95-1-0367

6. AUTHOR(S)
April S. Brown

7. PERFORMING ORGANIZATION NAME(S) AND ADDRESS(ES)
eorgia Institute of Technology
Atlanta, GA 30332

8. PERFORMING ORGANIZATION REPORT NUMBER

9. SPONSORING / MONITORING AGENCY NAME(S) AND ADDRESS(ES)
U. S. Army Research Office
P.O. Box 12211
Research Triangle Park, NC 27709-2211

10. SPONSORING / MONITORING AGENCY REPORT NUMBER
ARO 34434.8-PH

11. SUPPLEMENTARY NOTES
The views, opinions and/or findings contained in this report are those of the author(s) and should not be construed as an official Department of the Army position, policy or decision, unless so designated by other documentation.

12 a. DISTRIBUTION / AVAILABILITY STATEMENT
Approved for public release; distribution unlimited.

12 b. DISTRIBUTION CODE

13. ABSTRACT (Maximum 200 words)

Strain-Modulated Epitaxy (SME) is a novel approach, invented at Georgia Tech, to utilize subsurface stressors to control strain and therefore material properties and growth kinetics in the material above the stressors. The stressors are induced by patterning and compliant bonding in a composite substrate. The goal of this effort is to explore implementations and applications for and resulting from this new technique. We have (1) invented the first use of metal bonds and bonded substrate removal for SME; (2) developed metastable growth and finite element mechancal models for SME; (3) grown mismatched materials on metal bonded substrates, (4) observed new growth kinetics and the alignment of mounds on bottom-patterned substrates, (5) observed the control of strain in self-assembled quantum dots with anion exchange; and (6) invented a new in-situ compliant substrate bond approach.

14. SUBJECT TERMS

15. NUMBER OF PAGES
17

16. PRICE CODE

17. SECURITY CLASSIFICATION OR REPORT	18. SECURITY CLASSIFICATION ON THIS PAGE	19. SECURITY CLASSIFICATION OF ABSTRACT	20. LIMITATION OF ABSTRACT
UNCLASSIFIED	UNCLASSIFIED	UNCLASSIFIED	UL

(1) List of Illustrations and Tables

(1) Statement of the Problem Studied: Strain-Modulated Epitaxy (SME) is a novel approach, invented at Georgia Tech, to utilize subsurface stressors to control strain and therefore material properties and growth kinetics in the material above the stressors. The stressors are induced by patterning and compliant bonding in a composite substrate. The goal of this effort is to explore implementations and applications for and resulting from this new technique. (Work also supported by ONR MURI on Compliant Substrates).

(2) Summary of the Most Important Results

Definition and Objective

The objective of this project is to develop a fundamentally new technique for producing quantum-confined photonic devices by MBE with compliant substrates. A compliant substrate is defined as a substrate which is not rigid, but can instead conform to the lattice constant of a mismatched overlayer, when necessary. When mismatched epitaxial layers are grown on them, the lattice constants of compliant substrates can compress or expand to accommodate part of the total strain of the system. Because some of the strain is transferred to the compliant substrate, a thicker strained epitaxial layer can be grown and the critical thickness of that layer is extended.

Since the strain in the epitaxial layer can be reduced with a compliant substrate, a patterned compliant substrate can be used to achieve a lateral strain profile in the epitaxial film. The pattern in the compliant substrate modulates the overlayer-to-substrate thickness ratio, and the strain at the surface of the epitaxial film is thus laterally controlled by the ratio. Therefore, such a strain variation could lead to significant lateral changes in the In composition, and therefore thickness, of the film *without any surface patterning or post-growth processing*.

Additionally, growth kinetics that are dependent on strain can also be used to realize further lateral material property variation. Such effects are numerous. They include indium desorption, migration of adatoms, two- to three-dimensional growth mode transition thickness and the movement and formation of As precipitates. The growth kinetics that depend on strain can be emphasized or de-emphasized by the choice of growth conditions. This technique can be viewed as an inverted stressor approach, in

which the three-dimensional geometry of a strained bilayer modifies the material deformation plus the additional *and significant* effects realized by growth kinetic modifications.

Key Achievements

Development of the **Bonded Substrate Removal Process**

Although epitaxial lift-off with contact bonding is widely used for a variety of applications and was an important stepping stone in the initial work on the thin film compliant substrates, a great effort was made to move towards a compliant substrate made using bonding with subsequent substrate removal. There are two important reasons why bonded substrate removal is a better fit to the long term goals of the compliant substrate project. Substrate removal enables the fabrication of larger area substrates, since this technique does not rely on the lateral etching of material - a process which is necessary for ELO. Additionally, the bottom patterned compliant substrates necessary for strain-modulated epitaxy can be made using the bonded substrate removal process without the transfer and inversion necessary when ELO is used with contact bonding. Although ELO could be used for the bottom patterned compliant substrates by first bonding the sample to a mechanical host substrate, as in the bonded substrate removal process, the procedure is complicated by the fact that HF acid, which is used to laterally etch the sacrificial layer, also etches all of the bonding materials used in this work. Therefore, a great deal of time and effort was spent on the bonded substrate removal process which is shown below.

The as-grown material for both processes consisted of 2000 Å AlAs or high composition $Al_yGa_{1-y}As$ followed by a 2 μm GaAs layer for the thin film substrate. All of the material was grown by MBE on conventional GaAs substrates.

For the substrate removal process, the GaAs samples (4 mm - 1 cm on a side) were first mechanically lapped to a thickness of around 100 μm (Figure 1a). The GaAs samples were then bonded to the host substrate using a bond consisting of metal and metal diffusion barrier layers, (Figure 1b). The remainder of the substrate was then removed from the sample using a combination of citric acid:H_2O_2 and NH_4OH:H_2O_2 etches (Figure 1c), and the AlAs layer was transformed into an oxide with a low solubility in the etchant. The citric acid:H_2O_2 etch was first used as a static etch to remove the majority of the substrate material. The sample was left in the citric acid:H_2O_2 etch for several hours (etch rate ~ 7000 Å/min). The NH_4OH:H_2O_2 etch was used to remove the last few microns of substrate material. The NH_4OH:H_2O_2 is a fast etch, and therefore does not give the AlAs-oxide time to densify (less strained to remaining GaAs material). After the GaAs substrate was etched away, the sample was dipped in a 10% HF solution to dissolve the AlAs oxide (1d).

A great deal of process development went in to the creation of the bonded substrate removal process. Issues that were addressed include the selectivity of the etches, the selectivity mechanisms, and the surface morphology of the final substrate. The GaAs compliant substrates made using bonded substrate removal are bigger, more uniform, and more reproducible than those made by the ELO process. Substrates up to 1 cm^2 have been made using this process. At first, however, the compliant substrates that were made using

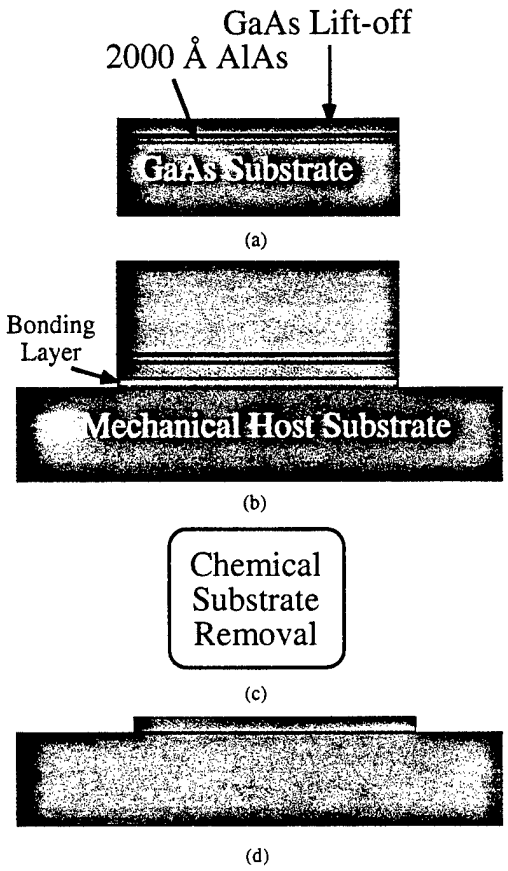

Figure 1. Bonded Substrate Removal Process Flow

this process had an inherent surface roughness. This microscopic roughness was thought to be due to the interface roughness often present when AlAs layers are grown on GaAs. This roughness has been alleviated in later experiments by smoothing this interface. This smooth surface morphology was obtained by growing high composition AlGaAs instead of AlAs and growing the Al containing layers at higher temperature. Atomic force microscopy has shown that the surface of the compliant substrate after growth is smooth on the atomic level. Difficulties have and do persist in reproducible bonding with metals. Metals (In/Ga) have appropriate viscosity and are compatible with MBE growth process. In addition to the metal bonds we also investigated the use of oxide bonds (see Figure 2) fabricated in conjunction with the University of Wisconsin (with Professor T. Kuech). In additon, an *in-situ* approach is under development at the end of this project and supported by an ONR on Compliant Substrates.

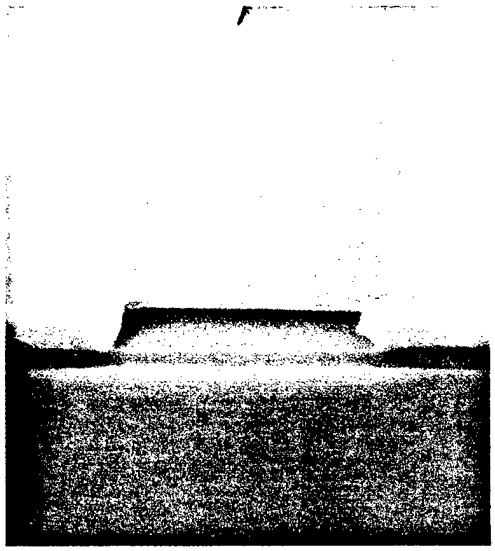

Figure 2. SEM of Glass Bonded Compliant Substrate

First Experiments Using Compliant Substrates Made by Bonded Substrate Removal

$In_{0.07}Ga_{0.3}As$ films were grown on GaAs substrates in five consecutive experiments. The epilayers were grown simultaneously on GaAs thin film compliant substrates, conventional GaAs substrates, and a piece of the as-grown compliant substrate material before bonding and substrate removal to compare strain accommodation. The compliant substrates were etched to ~3000Å before growth. The chosen thicknesses of the $In_{0.07}Ga_{0.93}As$ layers ranged from below to above the critical thickness on the conventional substrate. Nomarski microscope images were used to observe misfit dislocations on the samples and the x-ray diffraction spectra peak separations were used to determine the degree of relaxation. Differences in surface morphology and x-ray indications of strain-relaxation indicated that the InGaAs on the compliant substrates relaxes at a slower rate than the InGaAs on the reference substrates. A decrease in peak separation for layers grown on compliant substrates indicates that strain has been relieved. This can either be due to strain partitioning or relaxation through misfit dislocations. On the reference substrates, strain relief can only be caused by the creation of misfit dislocations. However, the FWHM for the InGaAs on the compliant substrates increases with increasing thickness for layers above 4000 Å. One possible explanation for this effect is a dramatic decrease in film quality in layers above 4000 Å thick. This does not appear likely in light of the x-ray peak intensity data. In fact, the peak intensity for the 8000 Å thick InGaAs on the compliant substrate is four times greater than that on the reference, and the FWHM for the GaAs peaks are comparable on the compliant and reference substrates. These first experiments for metal bonds indicate signficant differences in growth mode on compliant substrates. Similar results appear for other bond types, but one cannot eliminate the role of extrinsic compliant substrate processing issues.

Critical Thickness Modeling

Critical thickness is often used to provide an additional design constraint for growing dislocation free mismatched materials. Compliant substrates will have different critical thickness constraints because of strain partitioning with the substrate. Critical thickness modeling was used to generate critical thickness curves for several compliant substrate thicknesses to gain insight into the properties of compliant substrates. Experimental strain relief data was used for a Dodson-Tsao metastability model, and the final curves were compared to experimental compliant substrate data.

Figure 3 shows plots of the critical thickness curves overlaid with the experimental growth thicknesses. The thicknesses of the compliant substrates that were used in the experiment are written above each data point. By comparing the data with the critical thickness curve that matches the compliant substrate thickness that was used, it can be seen that, in all cases, the theory matches what was experimentally observed.
For example, in the $In_{0.04}Ga_{0.96}As$ growths on 6000 Å compliant substrates, no signs of relaxation were seen on either the 1500 Å or the 2500 Å epitaxial layer. These points lie well below the curves for both the 5000 Å and the 10000 Å compliant substrates. On the other hand, for the $In_{0.1}Ga_{0.9}As$ growths, the 4000 Å layer on the 5000 Å compliant substrate showed some signs of relaxation, while the 2000 Å layer on the 2500 Å compliant substrate did not. It can be seen in Figure 3 that the 4000 Å layer lies above the critical thickness curve for a 5000 Å compliant substrate, while the 2000 Å layer lies well below the critical thickness curve for a 2000 Å compliant substrate.

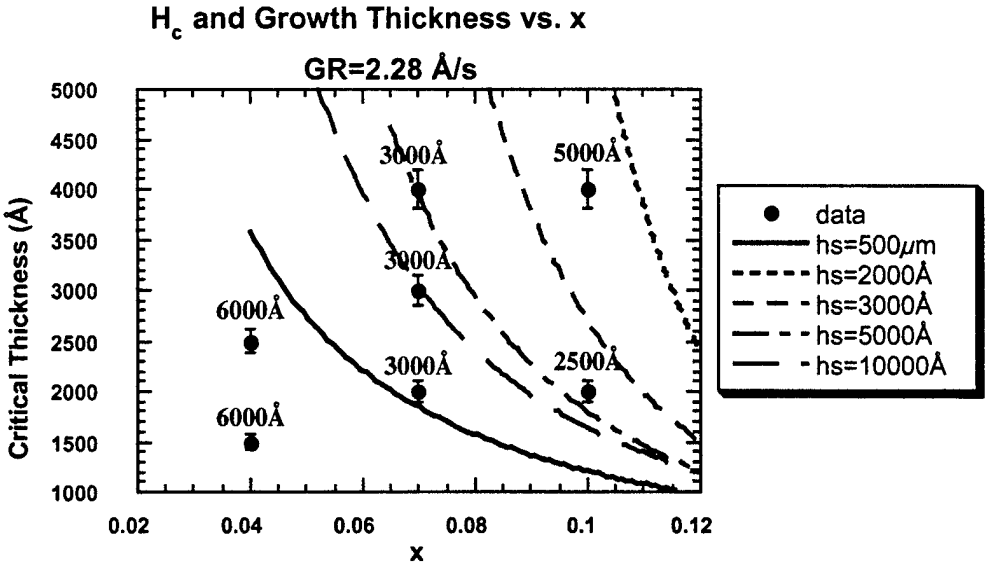

Figure 3. Model and Experiment for Growth on Compliant Substrates

Finite Element Modeling for Bottom Patterned Compliant Substrates

Finite element modeling studies have been performed for the strain-modulated epitaxy project to better understand the effects of the pattern on the strain in the resulting layer. This technique predicts the effect of strain partitioning and pattern size and geometry. The insight gained from this modeling can then be coupled with strain-dependent growth kinetics to accurately model strained growth on bottom patterned compliant substrates.

The technique of employing a bottom patterned compliant substrate can be compared to the inverse of using stressors on the top surface to create strain in the layers below. Therefore, the effects of stress and strain in these substrates can be modeled in an inverted stressor approach using finite element modeling.

As an example of the models generated, graphs of strain in x for the three stripe geometries are shown in Figure 4. For the strain in the x-direction, the strain in the epilayer is negative while the strain in the compliant substrate is positive. This is what is expected, since the epitaxial InGaAs has a larger lattice constant than the GaAs substrate. For the 10 μm stripe, it appears that the strain in each of the parts of the pattern are completely decoupled, whereas for smaller stripe widths there is an increasing coupling between them. The pattern plays an increasing role in the properties of both layers as the pattern width gets smaller. For the 10 μm stripe in the x-direction, the strain is 3.3×10^{-3} and 4.5×10^{-3} in the 2000 Å thick and 4000 Å thick regions of the substrate, respectively. Using the partitioning formula, the ratio of the strain is exactly what is expected for a 2500 Å $In_{0.1}Ga_{0.9}As$ layer grown on a bottom patterned compliant substrate with these thicknesses. Since the finite element model uses only material parameters to calculate the strain, this confirms that the partitioning formula is indeed correct.

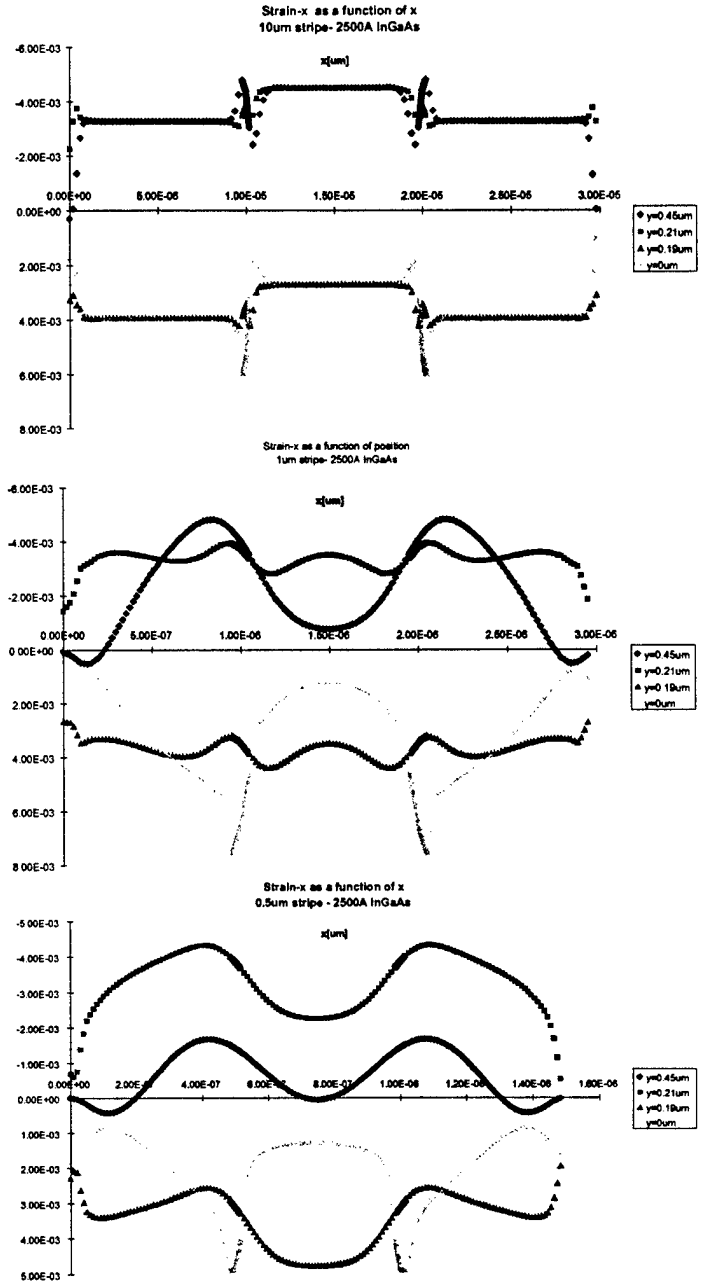

Figure 4. Finite element modeling results in the x-direction for a structure with a stripe width of 10 μm (top), 1 μm (middle), and 0.5 μm (bottom). The effect of the pattern becomes larger as the pattern width is decreased. l y=0.45 μm, n y=0.21 μm, s y=0.19 μm, and 8 y=0.0 μm.

DMS (Desorption Mass Spectrometry) Experiments

Our approach depends on the exploitation of strain-dependent growth kinetics. MBE growth kinetics are not well quantified. In order to begin characterizing growth kinetics, we measured and then modeled the dependence of In desorption on growth parameters during InGaAs growth on GaAs. In order to do this, we utilized the technique of Reflection Mass Spectrometry (RMS).

A UTI mass spectrometer was positioned in a line-of-sight to the substrate holder via an apertured nipple. We grew InGaAs/GaAs structures and related the In signal detected by the mass spectrometer to desorbed In. The desorption spectra (In signal vs. time) were recorded as a function of growth temperature (510-630 °C), indium composition (5-21%), InGaAs growth rate (0.43-0.9 μm/hr), V/III beam equivalent pressure ratio (17:1, 36:1) and arsenic species (As_4, As_2). A number of important findings related to InGaAs growth kinetics were made. First, we observed two distinct desorption mechanisms from analysis of the desorption spectra. The relative importance of these two growth regimes depends on the As to Group III flux ratio. An activation energy for one of the mechanisms was determined to be 1.3 eV.

We find that this activation energy is independent of growth kinetics. However, we do find that the composition of In in InGaAs depends significantly on growth conditions. The resultant composition in a growing film is determined by the interplay of desorption, surface population and incorporation. In this study, we quantified incorporation kinetics and surface concentration as a function of growth kinetics. The incorporation activation energy as a function of growth kinetics. The incorporation activation energy depends on InGaAs growth rate and on As species. A significant increase in incorporation is observed with the use of As_2 rather than As_4. The dependence of the incorporation kinetics on InGaAs growth rate may be exploited in strain-modulated epitaxy to obtain lateral composition variation.

Strain-Modulated Epitaxy Experiments

We observed for the first time that the pattern perturbed the growth and that defect spatially aligned themselves with the stripes at high growth temperatures. In these experiments, thin layers of 2500 Å $In_{0.07}Ga_{0.93}As$ were grown on GaAs patterned thin film substrates with various pattern geometries and thick GaAs reference substrates in a Riber 2300 MBE with various substrate temperatures. Each experiment contained at least three patterned thin film substrates with three different pattern geometries and a conventional GaAs substrate. The patterns were stripes 5-15 μm in width (separated by the same amount), oriented along the (011) and (01$\bar{1}$) directions and ~100 μm circles spaced 300 μm apart. As in the first bottom patterned compliant substrate experiment, the compliant substrates were etched to ~4000 Å and ~2000 Å in each of the regions. InGaAs 2500 Å thick was grown on the GaAs bottom patterned compliant substrates and GaAs reference substrates simultaneously. After the oxide desorption, a GaAs buffer layer was grown for 3 minutes to smooth the substrate surface. Four growths were performed in which the InGaAs growth temperature was varied and all other parameters were kept constant. $In_{0.07}Ga_{0.93}As$ was grown at 0 °C, 20 °C, 40 °C and 60 °C below the oxide

desorption temperature (assumed to be 580 °C, 560 °C, 540 °C and 520 °C, respectively). The substrate was ramped up to the growth temperature over 30 minutes and ramped down to room temperature in 20 minutes. Double crystal x-ray diffraction on the references showed that the sample grown at 520 °C had a peak separation of 1360 arc-sec, corresponding to 7% In content. The samples grown at 560 °C and 580 °C had peak separations corresponding to 2.5% In and 1.2% In, respectively. This implies In desorption of 64% and 84%, respectively. The samples were also characterized using Nomarski microscopy, low temperature photoluminescence and AFM.

The substrates were mostly intact after growth, though the MBE preparation etch resulted in some of the substrate being etched away. Nomarski microscopy was used to observe the surface morphology of the layers grown on the bottom patterned compliant substrates and reference substrates. There was no sign of misfit dislocations, by design, on any of the samples. In all cases, the InGaAs grown on the reference substrates exhibited a clear, featureless surface except for a low density of mounds. The InGaAs grown at 520 °C on the bottom patterned compliant substrate also was smooth except for a low density of mounds. A slight height variation could also be seen. The InGaAs films grown at 560 °C and 580 °C have a large density of mounds oriented in the $(01\bar{1})$ direction which increase in density with increasing temperature.

Theta/2theta double crystal x-ray diffraction of the reference samples (Figure 5) shows that the InGaAs peak shifts closer to the GaAs substrate peak with increasing growth temperature. This indicates that the indium in the sample decreases from 7% for the samples grown at 520°C to only 0.5% for the samples grown at 580°C.

Figure 6 shows AFM pictures of the three compliant substrates with $(01\bar{1})$ oriented stripes. Once again, the increasing density of the mounds is very noticeable. The surface

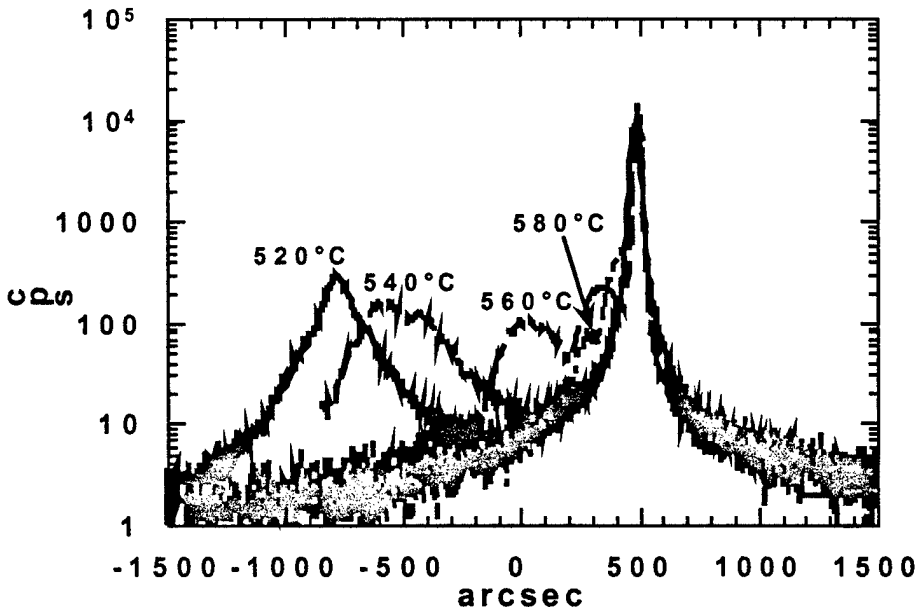

Figure 5. Theta/2theta x-ray scans of reference samples. The indium percentage in the layer decreases from 7% in the sample grown at 520 °C to 0.5% in the sample grown at 580 °C.

morphology of the sample grown at 520 °C (Figure 5 left picture) is atomically smooth with an average roughness of 3 Å in the areas between the mounds. This reconfirms the high quality of the Ga metal bond. Also notable is the average thickness variation across the substrate on each of the three samples. On the sample grown at 520 °C, the average height variation from region to region is 350 Å. On the sample grown at 560 °C, the average height variation is 720 Å, and the sample grown at 580 °C has an average variation of 1000 Å.

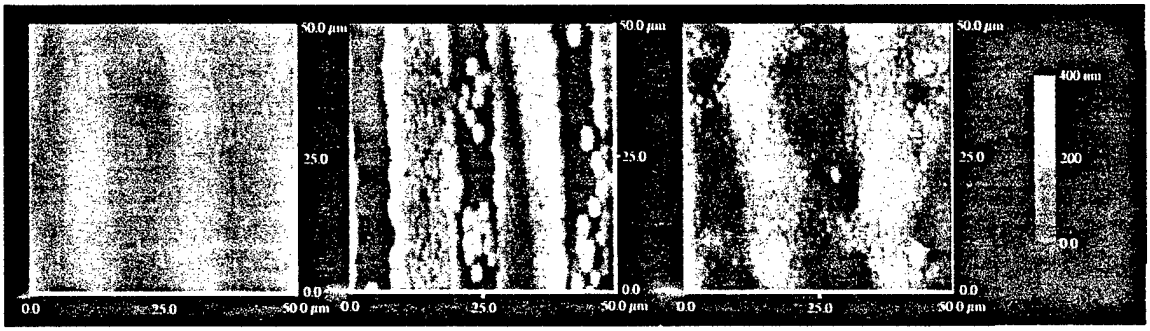

Figure 6. AFM images of growth on bottom patterned compliant substrates with $(01\bar{1})$ oriented stripes at growth temperatures of 520 °C (left), 560 °C (middle), and 580 °C (right).

Figure 7 shows the mound density on the compliant substrates and the references as a function of temperature. The low density of mounds on the reference substrates decreases with increasing temperature until they are not even detectable at 580 °C. The mound density on the bottom patterned compliant substrates, however, increases with increasing temperature. Mounding has been seen in both homoepitaxial growth and in highly strained heteroepitaxial growth. It is thought that, in the type of mounding seen in homoepitaxy, mound formation is due to an unstable growth mode which occurs when the terrace width is larger than the distance that the adatoms travel before nucleating an island. Mounding then occurs when the kinetic barrier at the edge of island is high enough that adatoms which land on top of the island do not have enough energy to migrate off of the island and instead nucleate on top of the island. When the growth temperature is increased, the adatoms are more likely to have the kinetic energy necessary to overcome the island step edge barrier. Thus, with increasing temperature, the island density would decrease and eventually become negligible. This is what is seen for the mounds on the reference substrates.

Strain-induced islanding, on the other hand, is the observed precursor to three-dimensional Stranski-Krastanov growth. This type of mound formation is dependent on growth kinetics and strain. Although the mound behavior observed in these experiments has never been observed before, it is speculated that the island formation is due to strain-induced island formation in the striped regions of the InGaAs grown on the bottom patterned compliant substrates. It is possible that the pattern has affected the migration of the adatoms so that the growth kinetics in certain regions of the sample were ideal for mounding.

Higher magnification in the AFM images reveals a much smaller structure on the mounds of the samples grown at 580 °C on bottom patterned compliant substrates. Figure 8 shows high resolution height and phase images of these mounds. Very small structures are aligned along the terraces on one side only of the mounds on both of the samples. These structures have an average height of 50±20 Å. Additionally, there is one larger structure located in the middle of each of the mounds. This larger structure has an average height of 100 Å. A three-dimensional AFM image showing both of these structures is shown in Figure 9. It may be that the high density of dots that forms on the sides of the mounds result from a different mechanism than the solitary dot found in the middle of each mound. These dots were found on the mounds in both areas of the patterned compliant substrate with $(01\bar{1})$ oriented stripes, but only in one region of the (011) oriented stripes. All three of these areas had the highest density of mounds.

While the height of the images is close to the true value, the width of the object shown on the AFM image is a convolution of the AFM tip with the object. Therefore, the

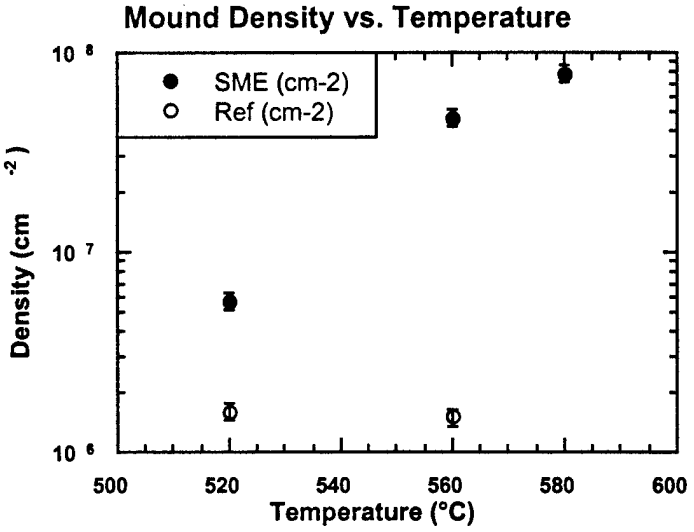

Figure 7. Mound density vs. temperature for the compliant substrate and reference samples.

object is likely more narrow than it appears. Quantum dots created by the Stranski-Krastanov growth method are typically 70-100 Å in height. This is comparable to the structures observed on the bottom patterned compliant substrates.

Following the speculation for strain induced mounding on the bottom patterned compliant substrates, it follows that eventually the strain would become so great that it would be energetically favorable to form small three-dimensional structures, or quantum dots. It is possible, then, that the dots only form on one side of the islands either because adatom migration is enhanced in that direction or because the strain is inherently higher on one of the two faceted sidewalls of the mound.

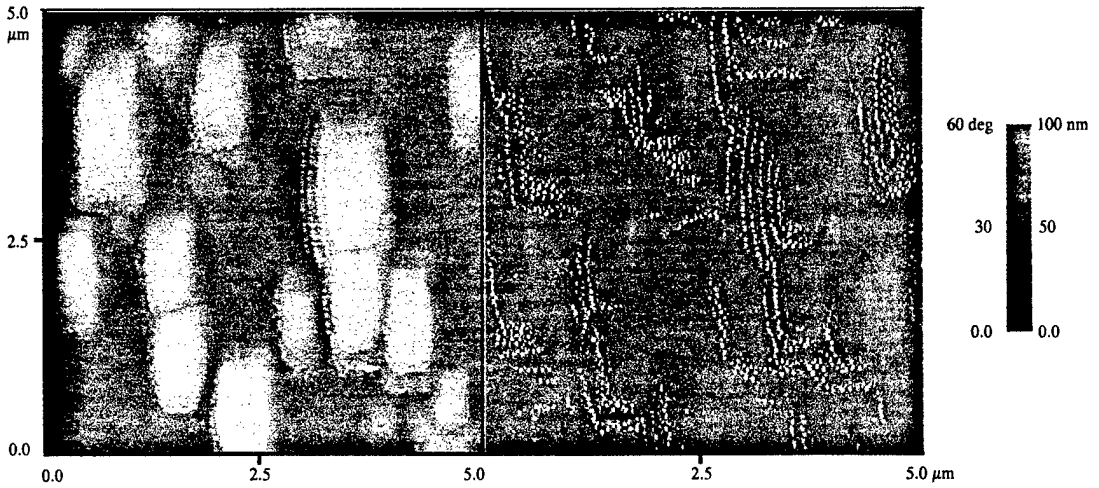

Figure 8. AFM height (left) and phase (right) images of mounds and dots on $(01\bar{1})$ oriented stripe patterned compliant substrate.

In conclusion, strain-modulated epitaxy experiments have been performed on bottom patterned compliant substrates. Lateral modulation in material thickness is seen at all growth temperatures, and, at temperatures where strain-dependent growth kinetics are significant, the bottom pattern compliant substrate affected the growth of strained epitaxial layers. The bottom patterned compliant substrate also causes mounds spatially aligned along the pattern. A new type of mounding mechanism is seen on the layers grown on bottom patterned compliant substrates, and it is speculated at these mounds, and the quantum dots that appear at the highest growth temperatures are caused by strain-dependent growth kinetics.

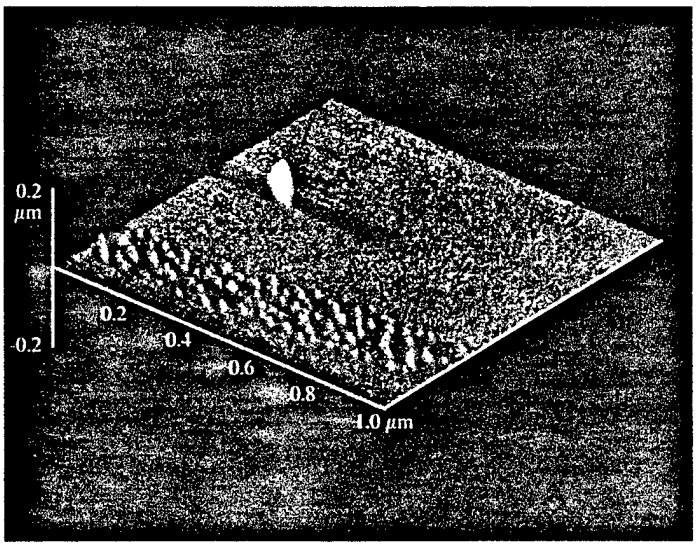

Figure 9. Three-dimensional AFM image of quantum dots oriented along edge of mound and in the middle.

Quantum Dot Formation and Annealing

In addition to the processing experiments, we are investigating the use of dissimilar anion annealing on quantum dot morphological evolution and control. This is to better understand the Skranski Krastinov growth mode and how self-assembled quantum dots may be better controlled by SME. Annealing may allow for better strain control via diffusion after growth. It is important to understand the issues associated with annealing and how overpressures can control material exchange. We therefore investigated the formation of an InAsP surface on InAs dots by allowing a P_2 beam to impinge on InAs dots after growth. The exchange of P for As is enhanced at high temperature and can be observed by the changes in the RHEED pattern during anneal. Figure 10 shows the change in dot morphology with application of a phosphorus beam.

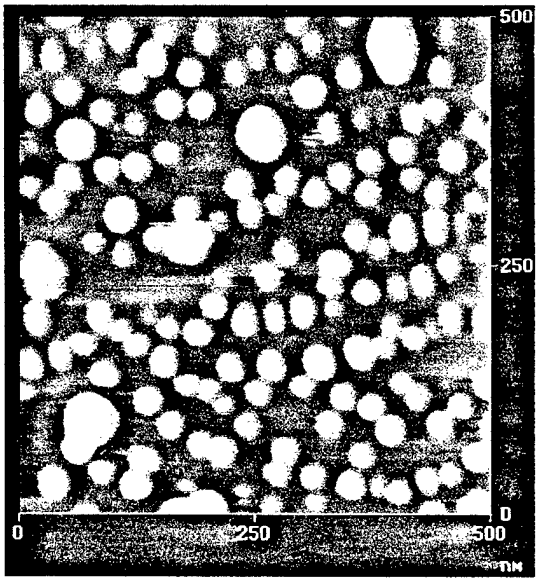

Fig. 10(a). InAs quantum dots with no anneal

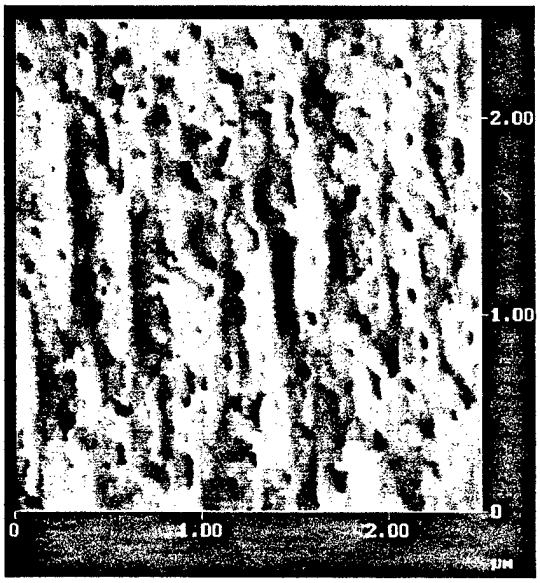

Fig. 10(b). InAs quantum dots with P_2 anneal at 500°C

***In-Situ* Bond:** We are currently developing a new approach which eliminates the nefor bonding. In this project we deposit an engineered metal bond (Al-Si eutectic, for example, in the MBE and then amorphous material above it. This elimates the bonding step and therefore may improve reproducibility in the process. This effort is supported in an ONR MURI program.

Publications:

(3) LIST OF REFEREED MANUSCRIPTS SUBMITTED OR PUBLISHED UNDER ARO SPONSORSHIP

1. Carter-Coman, C.A., Brown, A.S., and Jokerst, N.M., "Analysis of InGaAs layers on GaAs compliant substrates by double crystal x-ray diffraction," Appl. Phys. Lett. 70 (13), pp. 1754-1756, June 1997.

2. Fournier, F., Brown, A.S. Carter-Coman, C., Metzger, R.A., Doolittle, A., and Jokerst, N., "Growth Dynamics of InGaAs-GaAs by MBE," Journal of Crystal Growth, 175/176, pp. 203-210, May/June 1997.

3. Bicknell-Tassius, R., Brown, A.S., Lee, K., and May, G., "Application of Design of Experiments to InGaAs-GaAs Growth by MBE," Journal of Crystal Growth, 175/176, pp. 1131-1137, May/June 1997.

4. Kromann, R., Bicknell-Tassius, R., Lee, K., Brown, A.S., and Dorsey, J. "Real Time Monitoring of RHEED using Machine Vision Techniques," Journal of Crystal Growth, 175/176, pp. 334-339, 1997.

5. Carter-Coman, C.A., Bicknell-Tassius, R. Benz, R., Brown, A.S., and Jokerst, N., "Analysis of GaAs Substrate Removal Etching with Citric Acid: H_2O_3 and NH_4OH: H_2O_2 for Application to GaAs Compliant Substrates," Journal of the Electrochemical Society, 144, 2, pp. L29-L31, 1997.

6. Carter-Coman, Carrie, Bicknell-Tassius, Robert, Brown, April S., and Jokerst, Nan-Marie, "Metastability Modeling of Compliant Substrate Critical Thickness using Experimental Strain Relief Data," Appl. Phys. Lett. 71 (10), pp. 1344-1346, 8 September. 1997.

7. Carter-Coman, Carrie, Brown, April S., Metzger, Robert A., Jokerst, Nan Marie, Pickering, Jason, and Bottomely, Lawrence, " A New Mechanism for Spontaneous Nanostructure Formation on Bottom-Patterned Compliant Substrates," Appl. Phys. Lett. 71 (19), pp. 2773-2775, 10 November 1997.

8. Shen, J.J., Brown, April S., Metzger, Robert A., Sievers, Barry, Bottomley, Lawrence, Eckert, Patrick, and Carter, Brent, W., " Modification of Quantum Dot Properties Via Surface Exchange and Annealing: Substrate Temperature Effects," accepted for publication in the Journal of Vacuum Science and Technology B. 16(3), pp. 1326-1329, May/Jun 1998.

9. Brown, A.S., "Compliant Substrates Technology: Status and Prospects," submitted to Journal of Vacuum Science and Technology, Journal of Vacuum Science and Technology B 16(4) July/Aug. 1998.

10. Carter-Coman, C., Brown, A.S., and Jokerst, N. M., "Compliant Substrates for Reduction of Strain Relief in Mismatched Overlayers," MRS Conference Proceedings, vol. 441, pp. 361-366, Boston, MA, November 1996.

(4) SCIENTIFIC PERSONNEL SUPPORTED BY THIS PROJECT AND DEGREES AWARDED DURING THIS REPORTING PERIOD

April S. Brown, Associate Professor
Nan Marie Jokerst, Associate Professor
Carrie Carter, received Ph.D 1997
J.J. Shen, Ph.D. Student

(5) REPORT OF INVENTIONS

None.